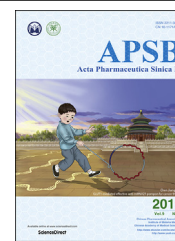




Chinese Pharmaceutical Association
Institute of Materia Medica, Chinese Academy of Medical Sciences

Acta Pharmaceutica Sinica B

www.elsevier.com/locate/apsb
www.sciencedirect.com



ORIGINAL ARTICLE

Ablation of gut microbiota alleviates obesity-induced hepatic steatosis and glucose intolerance by modulating bile acid metabolism in hamsters



Lulu Sun^{a,†}, Yuanyuan Pang^{a,†}, Xuemei Wang^a, Qing Wu^a,
Huiying Liu^a, Bo Liu^a, George Liu^b, Min Ye^c, Wei Kong^a,
Changtao Jiang^{a,*}

^aDepartment of Physiology and Pathophysiology, School of Basic Medical Sciences, Peking University, and the Key Laboratory of Molecular Cardiovascular Science, Ministry of Education, Beijing 100191, China

^bInstitute of Cardiovascular Sciences and Key Laboratory of Molecular Cardiovascular Sciences, Ministry of Education, Peking University, Beijing 100191, China

^cState Key Laboratory of Natural and Biomimetic Drugs, School of Pharmaceutical Sciences, Peking University, Beijing 100191, China

Received 12 October 2018; received in revised form 30 December 2018; accepted 18 January 2019

KEY WORDS

Gut microbiota;
CYP7B1;
T β MCA;
FXR;
Metabolic disorders

Abstract Since metabolic process differs between humans and mice, studies were performed in hamsters, which are generally considered to be a more appropriate animal model for studies of obesity-related metabolic disorders. The modulation of gut microbiota, bile acids and the farnesoid X receptor (FXR) axis is correlated with obesity-induced insulin resistance and hepatic steatosis in mice. However, the interactions among the gut microbiota, bile acids and FXR in metabolic disorders remained largely unexplored in hamsters. In the current study, hamsters fed a 60% high-fat diet (HFD) were administered

Abbreviations: ALT, alanine amino-transferase; ApoB, apolipoprotein B; AST, aspartate transaminase; AUC, area under curve; BAs, bile acids; BSH, bile acid hydrolase; CA, cholic acid; CAPE, caffeic acid phenethyl ester; CDCA, chenodeoxycholic acid; CETP, cholesterol ester transfer protein; CYP7A1, cytochrome P450 family 7 subfamily A member 1; CYP7B1, cytochrome P450 family 7 subfamily B member 1; CYP8B1, cytochrome P450 family 8 subfamily B member 1; CYP27A1, cytochrome P450 family 27 subfamily A member 1; DCA, deoxycholic acid; eWAT, epididymal white adipose tissue; FGF15/19, fibroblast growth factor 15/19; FXR, farnesoid X receptor; GCA, glycocholic acid; GCDCA, glycochenodeoxycholic acid; GTT, glucose tolerance test; HFD, high fat diet; H&E, hematoxylin and eosin; ITT, insulin tolerance test; LCA, lithocholic acid; NASH, non-alcoholic steatohepatitis; NAFLD, non-alcoholic fatty liver disease; PBA/SBA, primary bile acids to secondary bile acids; sWAT, subcutaneous white adipose tissue; TC, total cholesterol; TCA, taurocholic acid; T2D, type 2 diabetes; TG, triglycerides; T β MCA, tauro- β -muricholic acid; UDCA, ursodeoxycholic acid; UPLC–MS/MS, ultra performance liquid chromatography–tandem mass spectrometry; VLDL, very low-density lipoprotein

*Corresponding author.

E-mail address: jiangchangtao@bjmu.edu.cn (Changtao Jiang).

[†]These authors made equal contributions to this work.

Peer review under responsibility of Institute of Materia Medica, Chinese Academy of Medical Sciences and Chinese Pharmaceutical Association.

<https://doi.org/10.1016/j.apsb.2019.02.004>

2211-3835 © 2019 Chinese Pharmaceutical Association and Institute of Materia Medica, Chinese Academy of Medical Sciences. Production and hosting by Elsevier B.V. This is an open access article under the CC BY-NC-ND license (<http://creativecommons.org/licenses/by-nc-nd/4.0/>).

vehicle or an antibiotic cocktail by gavage twice a week for four weeks. Antibiotic treatment alleviated HFD-induced glucose intolerance, hepatic steatosis and inflammation accompanied with decreased hepatic lipogenesis and elevated thermogenesis in subcutaneous white adipose tissue (sWAT). In the livers of antibiotic-treated hamsters, cytochrome P450 family 7 subfamily B member 1 (CYP7B1) in the alternative bile acid synthesis pathway was upregulated, contributing to a more hydrophilic bile acid profile with increased tauro- β -muricholic acid (T β MCA). The intestinal FXR signaling was suppressed but remained unchanged in the liver. This study is of potential translational significance in determining the role of gut microbiota-mediated bile acid metabolism in modulating diet-induced glucose intolerance and hepatic steatosis in the hamster.

© 2019 Chinese Pharmaceutical Association and Institute of Materia Medica, Chinese Academy of Medical Sciences. Production and hosting by Elsevier B.V. This is an open access article under the CC BY-NC-ND license (<http://creativecommons.org/licenses/by-nc-nd/4.0/>).

1. Introduction

The human gut is a complex ecosystem consisting of 10–100 trillion bacteria. Accumulating evidences suggest that the gut microbiota is associated with metabolic diseases, including obesity¹, insulin resistance^{2,3} and non-alcoholic fatty liver disease (NAFLD)⁴. The drugs for type 2 diabetes (T2D) also produce therapeutic effects by modulating microbial homeostasis^{5–8}. The gut microbiota plays an essential role in the progress of metabolic diseases and is thus a potential drug target.

Dietary nutrients are the main drivers for remodeling the gut microbiota in the daily life of the host. In a cohort study, dietary fiber-induced improvement in glucose metabolism was due to the increased abundance of *Prevotella*⁹. Moreover, the content and diversity of gut microbiota in obese patients are lower than those in lean subjects¹⁰. Microbiota-derived metabolites, such as bile acids, short chain fatty acids and endotoxin, influence host metabolism by mediating the interaction between the gut and other organs¹¹. Recent studies identified a link between the imbalance of intestinal flora and the pathological changes in the metabolism of bile acids in patients suffering from obesity and type 2 diabetes^{5,12,13}. In the liver, cholesterol is converted to primary bile acids *via* two pathways, with cytochrome P450 family 7 subfamily A member 1 (CYP7A1) as the rate-limiting enzyme in the classic pathway and cytochrome P450 family 7 subfamily B member 1 (CYP7B1) as an important enzyme in the alternative pathway¹⁴. It was reported that CYP7B1-mediated activation of the alternative pathway exerted metabolic benefits by shaping the gut microbiota and upregulating cold-induced thermogenesis and energy expenditure¹⁵. Primary bile acids synthesized in the liver are conjugated to taurine and glycine for secretion into the gut. In the gut, the conjugated primary bile acids are deconjugated by bile salt hydrolase (BSH) in gut bacteria flora and 7 α / β -dehydroxylases, converting cholic acid (CA) and chenodeoxycholic acid (CDCA) to secondary bile acids, deoxycholic acid (DCA) and lithocholic acid (LCA), respectively¹⁶.

It is well established that bile acids bind to farnesoid X receptor (FXR), the nuclear receptor that is involved in the control of bile acid homeostasis and the enterohepatic circulation of bile acids and is known to influence multiple metabolic diseases^{16,17}. Activation of intestinal FXR induces fibroblast growth factor 15 (FGF15) to activate hepatic FGF receptor 4/ β -Klotho signaling to inhibit bile acid synthesis. Notably, recent studies in mice demonstrated that tauro- β -muricholic acid (T- β MCA) antagonizes intestinal FXR, inhibiting the FXR-FGF15 axis to influence hepatic bile acid and cholesterol metabolism^{18–20}, and that inhibition or ablation of intestinal FXR prevented obesity-related metabolic dysfunction in

high-fat diet (HFD)-fed and genetically obese mice^{21–23}. However, there are many differences in the bile acid composition between humans and mice, because humans only produce CA and CDCA in the liver whereas mice also produce ursodeoxycholic acid (UDCA) which therefore should be considered as primary bile acid in mice. Intestinal FXR signaling induces FGF15 in mice but FGF19 in humans, with a different regulation of CYP7A1 and cytochrome P450 family 8 subfamily B member 1 (CYP8B1)²¹, thus revealing the limitation of translational applications of studies performed in mouse models. Compared with mice, the hamster is considered to be a more appropriate model for studies of metabolic diseases²⁴. Notably, lipid metabolism in hamsters is more similar to that in humans, including the production of HFD-induced high plasma triglycerides, the levels of high cholesterol ester transfer protein (CETP) and very low-density lipoprotein (VLDL), and the specific apolipoprotein B (ApoB) expression in the intestine^{25,26}. The HFD-fed golden Syrian hamster model has been used as an animal model of insulin resistance, hepatic steatosis and dyslipidemia, as hamsters have similar lipid profiles to human and are predisposed to HFD-induced hyperlipidemia^{27–29}. Collectively, the hamster is a more ideal animal model to study the pathogenesis and pharmacological interventions of human diet-related metabolic diseases. In the current study, the metabolic phenotypes, bile acid metabolism and FXR signaling were examined after the ablation of the gut microbiota in hamsters.

2. Material and methods

2.1. Animals

Golden Syrian hamsters were purchased from the Beijing Vital River Laboratory Animal Technology Co., Ltd. Six- to eight-week-old male hamsters were housed in a standard SPF environment (12 h daylight cycle, lights off at 18:00). The hamsters were divided into two groups and given 0.5% CMC-Na (Sigma, St. Louis, MO, USA) or an antibiotic cocktail suspended in 0.5% CMC-Na by gavage twice a week under a 60% high-fat diet (D12492, Research Diet, New Brunswick, NJ, USA) treatment for 4 weeks. The combined antibiotics were consisted of vancomycin (50 mg/kg, Sigma), metronidazole (100 mg/kg, Sigma), kanamycin (100 mg/kg, Sigma) and ampicillin (100 mg/kg, Sigma). The antibacterial spectrum of each antibiotic is as follows (data from Antimicrobe.org):

Vancomycin: coagulase negative *Staphylococci*, *Streptococcus* spp., *Streptococcus pneumoniae*, *Staphylococcus aureus* (vancomycin susceptible), *Enterococcus* spp. (vancomycin-

susceptible), *Clostridium* spp., *Corynebacterium jeikeium*, *Listeria monocytogenes*, and *Actinomyces*.

Metronidazole: anaerobic Gram-negative bacilli including *Bacteroides* species, *Prevotella* spp.; *Fusobacterium* spp., *Porphyromonas* spp.; anaerobic Gram-positive bacilli including *Clostridium* spp.; Protozoa including *Blastocystis hominis*, *Entamoeba histolytica*, *Giardia lamblia*, and *Trichomonas vaginalis*; Anaerobic cocci including *Peptostreptococcus* species, *Veillonella* species.

Kanamycin: *Proteus* species (both indole-positive and indole-negative), *E. coli*, *Enterobacter aerogenes*, *Serratia marcescens*, *Klebsiella pneumoniae*, and *Acinetobacter* species.

Ampicillin: Gram-positive including *Enterococcus* spp., *Streptococcus* spp., and *Listeria monocytogenes*; Gram-negative including *Haemophilus influenzae*, *Salmonella* spp., *E. coli*, *Proteus mirabilis*, and *Shigella* spp.

Body weights and food intakes were recorded once a week. Glucose tolerance tests and insulin tolerance tests were conducted during 4th week. The hamsters were sacrificed after 4-h fasting at the end of the 4th week. All animal experiment protocols were approved by the Animal Care and Use Committee of Peking University (Beijing, China).

2.2. Metabolic assays

For the glucose tolerance test, the hamsters were fasted for 16 h overnight. The blood glucose at different time points (0, 15, 30, 60, 90 and 120 min) was measured with an Accu-Check glucometer (Bayer, Leverkusen, Germany) before and after glucose (2.5 g/kg) challenge. The insulin tolerance test was carried out after fasting for 6 h. Blood glucose was measured before (0 min) and after (15, 30, 60 and 90 min) intraperitoneal injections of insulin (1.5 UI/kg). Blood glucose levels during glucose and insulin tolerance tests were detected using blood from the tails. Blood samples were collected after fasting for 4 h to measure fasting blood glucose and insulin (Insulin ELISA kit, Alpcos, Salem, OR, USA) levels. HOMA-IR was calculated according to Eq. (1) to assess glucose homeostasis in hamsters.

$$\text{HOMA-IR} = \text{Fasting blood glucose (mmol/L)} \times \text{Fasting insulin } (\mu\text{UI/mL}) / 22.5 \quad (1)$$

2.3. Histological analysis

Liver tissues were fixed in 4% paraformaldehyde for 4–6 h, and paraffin sections were cut and stained by hematoxylin and eosin (H&E). Tissues embedded in OCT were cut to obtain liver frozen sections, which were stained by oil red O. A minimum of three discontinuous sections were evaluated for each sample, with more than three samples per group.

2.4. Lipid measurements

Total triglycerides (TG) and cholesterol (TC) in the liver and plasma were measured (TGKIT and TCKIT, BioSINO, Beijing, China) to evaluate hepatic steatosis and dyslipidemia. The degree of liver injury was estimated based on plasma alanine aminotransferase (ALT) and aspartate transaminase (AST) (ALT/GPTKIT and AST/GOTKIT, BioSINO, Beijing, China).

2.5. Real-time PCR analysis

The ileal epithelium and liver tissues were frozen in liquid nitrogen and stored at -80°C . The standard chloroform–isopropanol

extraction was applied to isolate total RNA from lytic tissues in Trizol reagent. cDNA was synthesized from 2 μg total RNA with a Reverse Transcription Kit (ABM, Richmond, Canada). The relative expression of genes was normalized to 18S rRNA. All of the primer sequences used in the real-time PCR are listed in Supporting Information Table S1.

2.6. Sample collection

The ileal epithelium was scraped from the lower 1/3 of the small intestine after washing with PBS. Fresh fecal samples were collected from the cecum.

2.7. Bile acid analysis

Ten milligrams each of feces from the cecum, liver and ileal epithelium tissues was dissolved in 100 μL double-distilled water and pulverized. The protein was precipitated with 300 μL methanol containing 0.1% ammonium hydroxide. The supernatants were collected for further analysis, and chlorpropamide (Sigma) was added as an internal standard to quantify bile acid levels. The bile acid concentrations in the supernatants were measured by a UPLC/Synapt G2-Si QTQF MS system (Water Corp, Milford, MA, USA) with an ESI source. An Acquity BEH C18 column (100 mm \times 2.1 mm i.d., 1.7 μm , Waters Crop, Milford, MA, USA) was used for chromatographic separation. The column temperature was 45 $^{\circ}\text{C}$, and the flow rate was 0.4 mL/min. The mobile phase consisted of a mixture of 0.1% formic acid in water and 0.1% formic acid in acetonitrile. A gradient elution was conducted, and MS detection proceeded in the negative mode. A mass range of m/z 50 to 850 was acquired.

2.8. Data analysis

GraphPad Prism version 7.0 (GraphPad Software, San Diego, CA, USA) was used for statistical analysis. The sample sizes were determined by power analysis using StatMate version 2.0 (GraphPad Software, San Diego, CA, USA). Experimental data were shown as the mean \pm SEM. The investigators involved in this study were not completely blinded in the animal experiments during sample collection and analysis. No data were excluded from the data analysis. A two-tailed unpaired Student's *t*-test was used for all comparisons of the hamster-related experiments. *P* values of less than 0.05 were considered significant.

3. Results

3.1. Antibiotic treatment alleviated hepatic steatosis, inflammation and glucose intolerance in HFD-fed hamsters

To explore the role of gut microbiota in influencing obesity-related diseases, hamsters under HFD treatment were treated with vehicle or antibiotic cocktail by gavage for four weeks. In antibiotic-treated hamsters, the liver weights and the liver weight to body weight ratios were both reduced (Fig. 1A and B). H&E and oil red O staining revealed a reduced accumulation of lipids in the liver of antibiotic-treated hamsters compared with the vehicle (Fig. 1C and D). Moreover, antibiotic treatment significantly decreased hepatic and plasma triglyceride levels (Fig. 1E and F). Consistent with that, qPCR analysis indicated that lipid synthesis in the liver was

downregulated in antibiotic-treated hamsters, while lipid uptake and oxidation had no changes (Fig. 1G). The reduced levels of plasma alanine aminotransferase (ALT) and aspartate transaminase (AST) further demonstrated the improvement in the liver injury after antibiotic treatment (Fig. 1H and I). Above results suggested that antibiotic treatment had beneficial effects in reducing hepatic lipid accumulation and liver injury under 60% HFD treatment in hamsters.

The glucose tolerance test (GTT) and insulin tolerance test (ITT) revealed that glucose intolerance and insulin resistance were substantially improved after antibiotic treatment (Fig. 2A–C). Antibiotic-treated hamsters displayed lower fasting serum insulin level and HOMA-IR than the vehicle (Fig. 2D–F). Antibiotic-treated hamsters were resistant to HFD-induced body weight gain (Supporting Information Fig. S1A and B). The fat mass and fat weight/body weight ratios of subcutaneous white adipose tissue (sWAT) and epididymal white adipose tissue (eWAT) were markedly decreased after antibiotic treatment, while there were no differences in brown adipose tissue (Fig. 2G and Fig. S1C). It was reported that cold-induced microbial alteration was beneficial for being in the sWAT, resulting in an ameliorative metabolic phenotype in mice³⁰. Indeed, the mRNA levels of thermogenic genes, such as *Ucp1* and *Elovl3*, were significantly elevated in the sWAT of antibiotic-treated hamsters (Fig. 2H). Food intake remained unchanged between vehicle- and antibiotic-treated hamsters (Fig. S1D). The above results highlighted the effects of gut microbiota on the progress of HFD-induced metabolic disorders in hamsters.

3.2. Modulation of bile acid synthesis in the liver by antibiotics

Bile acids are mainly synthesized in the liver *via* both classical and alternative pathways. The classical pathway is initiated by the rate-limiting enzyme CYP7A1, which accounts for approximately 75% of bile acid production under physiological conditions. CYP7B1 is mainly involved in the alternative pathway³¹. Moreover, the formation of bile acids involves multiple enzymes, including cytochrome P450 family 27 subfamily A member 1 (CYP27A1) and CYP8B1 (Fig. 3A). Recent studies revealed that the expression of CYP7A1, CYP27A1 and CYP7B1 was influenced by the gut microbiota in mice²⁰. However, it remains unknown whether bile acid synthesis is under microbial regulation in hamsters. There was no significant difference in hepatic content of cholesterol and total primary bile acids in the liver between the two groups (Fig. 3B and C). Antibiotic treatment significantly decreased glycocholic acid (GCA) levels and significantly increased T β MCA levels in liver (Fig. 3D and E). Alterations in the bile acid composition were associated with metabolic disorders in the clinic. It was reported that the ratio of 12 α -OH to non-12 α -OH bile acids (12 α -OH to non-12 α -OH BAs) was positively associated with insulin resistance and hyperlipidemia³² and that the ratio of primary bile acids to secondary bile acids (PBA/SBA) declined in non-alcoholic steatohepatitis (NASH) patients³³. In antibiotic-treated hamsters, the PBA/SBA ratio was markedly elevated, while there was a decrease in the ratio of 12 α -OH to non-12 α -OH BAs (Fig. 3F and Supporting Information Fig. S2A). The conjugation of bile acids was not different between the two groups (Fig. S2B).

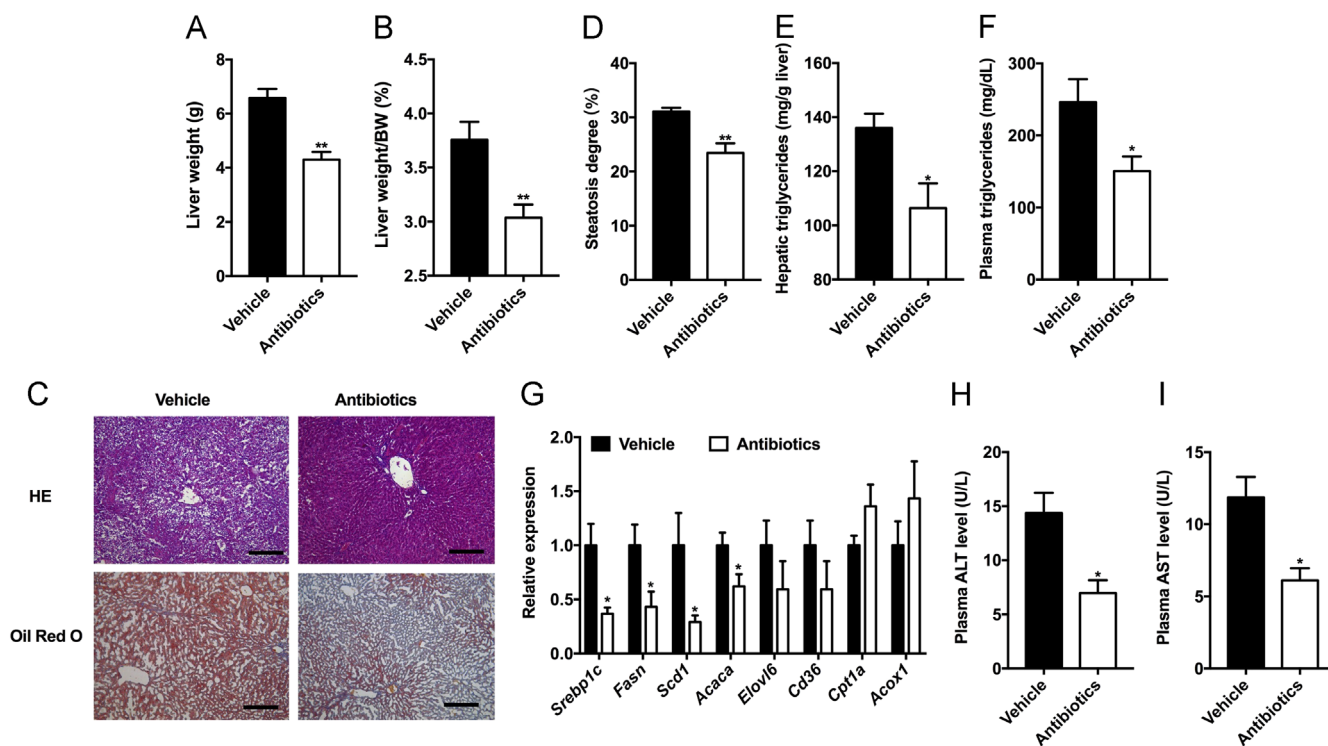


Figure 1 Ablation of gut microbiota protects from obesity-induced hepatic steatosis and liver injury in hamsters. The hamsters were fed a 60% high-fat diet and given vehicle or antibiotics for 4 weeks ($n=5$ hamsters/group). (A) The liver weight. (B) The ratio of liver weight to body weight. (C) Representative H&E (upper panel) and oil red O (lower panel) staining of liver sections of the two groups. Scale bars: 200 μ m (3 images/hamster). (D) Steatosis degree (the ratio of vacuolar area to whole area in one image, 3 images/hamster). (E) Hepatic triglycerides. (F) Plasma triglycerides. (G) The relative expression of genes involved in fatty acid synthesis, uptake and oxidation in the liver. (H) Plasma ALT levels. (I) Plasma AST levels. Data are presented as the mean \pm SEM. * $P<0.05$, ** $P<0.01$ versus vehicle by two-tailed Student's *t*-test.

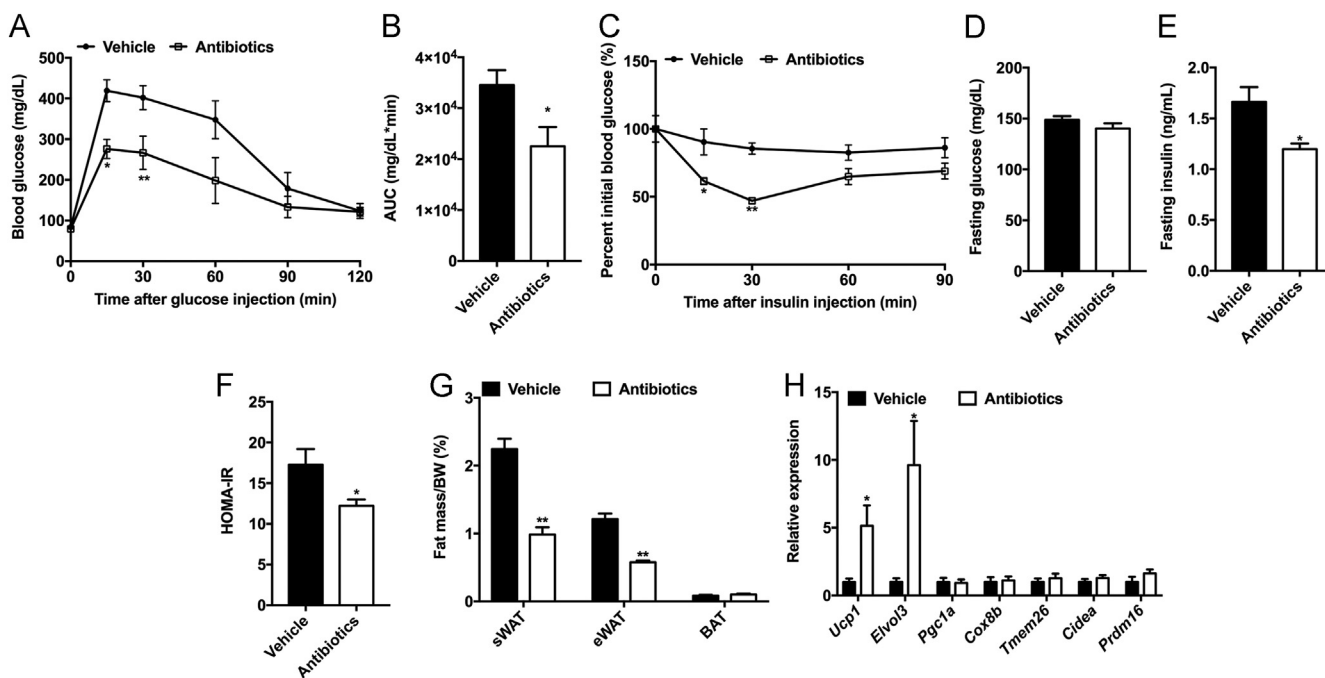


Figure 2 Ablation of gut microbiota improves obesity-induced insulin resistance in hamsters. The hamsters were fed a 60% high-fat diet and given vehicle or antibiotics for 4 weeks ($n=5$ hamsters/group). On the fourth week, glucose tolerance tests (GTT) and insulin tolerance tests (ITT) were performed. (A) GTT; (B) Area under the curve (AUC); (C) ITT. (D) Fasting glucose levels; (E) Fasting insulin levels; (F) HOMA-IR; (G) The ratios of fat mass to body weight in subcutaneous adipose tissue (sWAT), epididymal adipose tissue (eWAT) and brown adipose tissue (BAT); (H) The relative expression of thermogenic gene mRNAs in the sWAT. Data are presented as the mean \pm SEM, $n=5$ hamsters/group. * $P<0.05$, ** $P<0.01$ versus vehicle by two-tailed Student's t -test.

Furthermore, *Cyp7b1* mRNA was upregulated, while there were no significant changes in the relative expression of *Cyp7a1*, *Cyp27a1* and *Cyp8b1* (Fig. 3G). According to the hydrophobicity indices of bile acids, DCA, LCA, CA and their conjugates are hydrophobic, while β -muricholic acid (β MCA) and T β MCA are hydrophilic³⁴. In hamsters, gut microbiota depletion led to a more hydrophilic bile acid profile, with an elevation of T β MCA in the liver.

3.3. Antibiotic treatment remodeled the bile acid profiles in the gut

Multiple gut microbiota-derived enzymes are involved in bile acid modification, including deconjugation, transport and $7\alpha/\beta$ -dehydroxylation⁵. CA, CDCA and β MCA are produced from conjugated bile acids via BSH and are further converted to secondary bile acids after $7\alpha/\beta$ -dehydroxylation (Supporting Information Fig. S3A). The total ileal bile acid levels did not change after antibiotic treatment (Fig. 4A). Further metabolomics analysis showed that the levels of ileal and fecal secondary bile acids in the antibiotic-treated group were much lower than those in the vehicle-treated group, which was likely due to the absence of $7\alpha/\beta$ -dehydroxylase activity (Fig. 4B, C and Fig. S3C). Consistently, the ratio of PBA/SBA was significantly upregulated by antibiotic treatment (Fig. 4D and Fig. S3D). The reduction of total fecal bile acids was probably due to the deficient transformation from primary unconjugated bile acids to secondary bile acids (Fig. S3B). In the ileum, there was a reduced ratio of unconBA/conBA, with a remarkable accumulation of T β MCA (Fig. 4B, C and E), which was previously identified as an intestinal FXR antagonist in mice²⁰. The conjugated bile acids, such as glycochenodeoxycholic acid (GCDCA), GCA and

taurocholic acid (TCA), were more abundant in the feces of antibiotic-treated hamsters but there was no increase in the ileum, indicating the excretion of GCDCA, GCA and TCA was elevated after antibiotic treatment (Fig. S3C). The elevation in ileal T β MCA levels might have resulted from the increased CYP7B1-mediated synthesis and the decreased microbial deconjugation.

3.4. Antibiotic treatment suppressed intestinal FXR signaling

Inhibition of intestinal FXR exerted a protective role in insulin resistance and hepatic steatosis^{22,35}. T β MCA, the antagonist of intestinal FXR in mice, had been found to be markedly increased in the ileum of antibiotic-treated hamsters (Fig. 3D). In antibiotic-treated hamsters, FXR signaling was selectively suppressed in the gut but not in the liver (Fig. 5A and B). These results suggested that intestinal FXR inhibition was the potential target of gut microbiota-derived bile acid signaling in the metabolic diseases.

4. Discussion

Obesity, type 2 diabetes and non-alcohol fatty liver disease are aspects of metabolic syndrome, which is a major public health problem worldwide^{36–40}. Thermogenesis is considered a therapeutic target for obesity⁴¹. The progress of metabolic syndrome results from interactions between the gut microbiota and the host⁴². Some of these phenotypes could be transferred to germ-free mice by fecal transplantation from mice or patients^{43,44}. It was also found that the therapeutic effects in clinical treatment were determined by the composition of the gut microbiota in patients^{5,45,46}. Thus, a

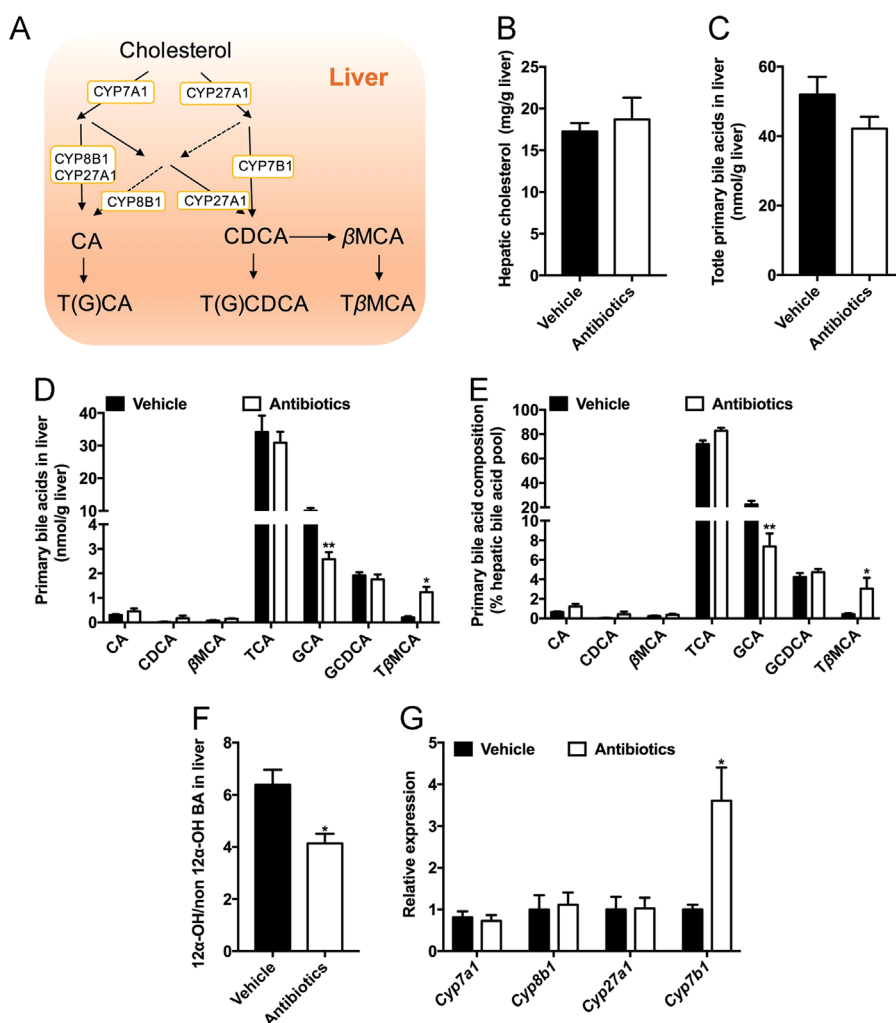


Figure 3 Alternative bile acid synthesis in the liver is elevated after antibiotic treatment. The hamsters were fed a 60% high-fat diet and given vehicle or antibiotics for 4 weeks ($n=5$ hamsters/group). (A) Bile acid synthesis in the liver; (B) Hepatic cholesterol; (C) Total primary bile acids in the liver; (D) Primary bile acid profiles in the liver; (E) Primary bile acid composition in the liver; (F) The ratio of 12 α -OH bile acids to non-12 α -OH bile acids in the liver [12 α -OH/non12 α -OH BA=(GCA+CA+TCA+GDCA+DCA+TDCA)/(LCA+HDCA+CDCA+UDCA+ β MCA+GCDCA+GUDCA+TLCA+TUDCA+THDCA+T β MCA)]; (G) The relative expression of genes involved in bile acid synthesis. Data are presented as the mean \pm SEM, $n=5$ hamsters/group. * $P<0.05$, ** $P<0.01$ versus vehicle by two-tailed Student's t -test.

more complete understanding of how the gut microbiota influences host metabolism and the development of novel therapeutic approaches are important research priorities. Previous studies demonstrated that mice on an HFD that were treated with antibiotics or tempol displayed reduced hepatic triglyceride accumulation and increased beiging of white adipose tissue. In the present study, another animal model, the golden Syrian hamster, was used to more accurately reflect metabolic dysfunction found in humans. There was an obvious hepatic lipid accumulation after only four weeks of HFD treatment. To evaluate the role of the gut microbiota in the progress of HFD-induced metabolic disorders, the HFD-treated hamsters were given vehicle or antibiotics by gavage twice a week for four weeks. After antibiotic treatment, the body weights and the percent of fat mass showed a significant reduction, accompanied by elevated expression of genes involved in thermogenesis in the sWAT. Furthermore, insulin sensitivity and hepatic steatosis were both ameliorated in the absence of the gut microbiota for hamsters on an HFD as a result of the inhibition of lipid synthesis in the liver.

Bile acids are metabolized in the gut, and the bile acid compositions vary widely among mice and humans. It is interesting to note that glycine-conjugated bile acids are much higher in hamsters than mice, which is more like humans. To further determine the microbial metabolism of bile acids in hamsters, a metabolomics analysis of liver, ileum and feces samples was performed. Due to the upregulated excretion in the feces, there was no significant change in the levels of hepatic and ileal GCDCA. In mice, but not in humans, CDCA is converted into α , β MCA through the activity of a sterol-6 β -hydroxylase, cytochrome P450, family 2, subfamily c, polypeptide 70 (CYP2C70), which is expressed in the mouse liver⁴⁷. In hamsters, antibiotic treatment markedly upregulated CYP7B1 expression, leading to a more hydrophilic bile acid composition with an increase in T β MCA and a reduction in GCA in the liver. CA feeding was shown to elevate fat absorption and aggravate glucose intolerance⁴⁸. A recent study showed that whole-body *Cyp7a1*-null (*Cyp7a1*^{-/-}) mice displayed an improvement of glucose tolerance and insulin sensitivity when fed an HFD⁴⁹.

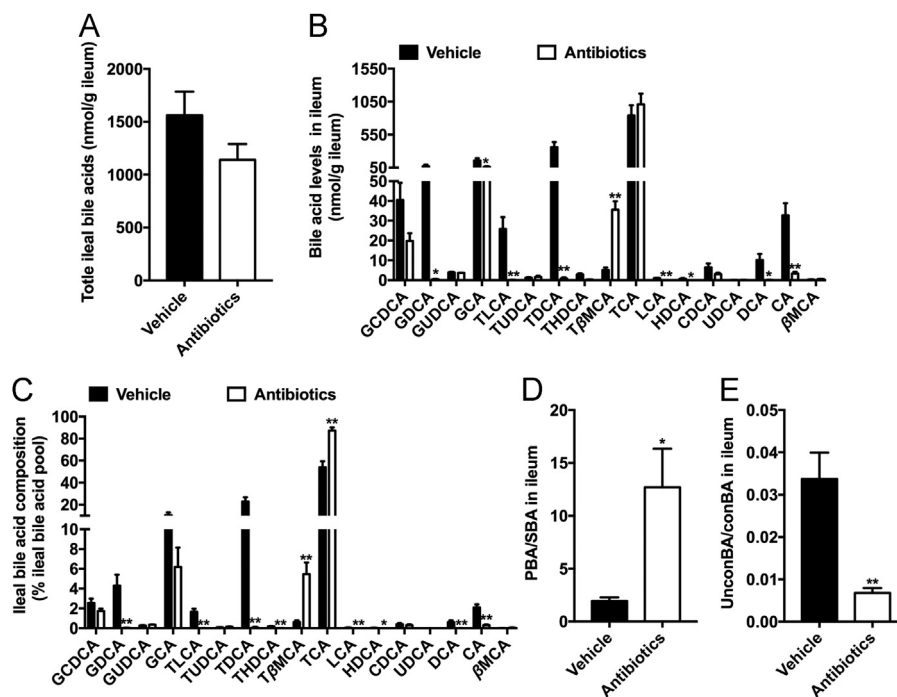


Figure 4 Microbial modulation of bile acid metabolism in the gut. (A) Total ileal bile acids; (B) Bile acid levels in the ileum; (C) Bile acid composition in the ileum; (D) The ratio of primary bile acids to secondary bile acids in the ileum; (E) The ratio of unconjugated bile acids to conjugated bile acids in the ileum. Data are presented as the mean \pm SEM, $n=5$ hamsters/group. * $P < 0.05$, ** $P < 0.01$ versus vehicle by two-tailed Student's t -test.

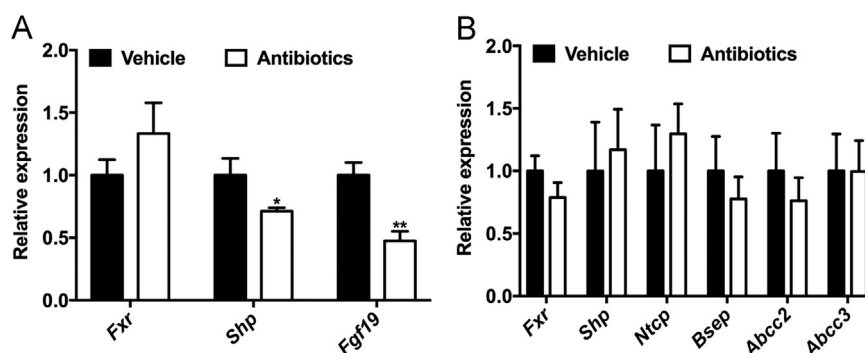


Figure 5 Intestinal FXR is suppressed in the absence of gut microbiota. (A) The relative abundance of intestinal FXR and its target genes; (B) The mRNA levels of genes in the hepatic FXR signaling. Data are presented as the mean \pm SEM, $n=5$ hamsters/group. * $P < 0.05$, ** $P < 0.01$ versus vehicle by two-tailed Student's t -test.

In *Cyp7a1*^{-/-} mice, the T β MCA content in bile was observed to increase as a result of CYP7B1 upregulation. T β MCA is the most efficacious endogenous FXR antagonist, and inhibition of intestinal FXR signaling was found to improve hepatic steatosis and insulin resistance^{8,22}. According to reported clinical data, hepatic CYP7B1 expression was down-regulated, while CYP7A1 and CYP8B1 expression remained similar in the obese individuals with type 2 diabetes (T2D) compared to health controls¹⁵. Moreover, cold-induced upregulation of CYP7B1 promoted thermogenesis and energy expenditure by increasing brown and beige adipocytes¹⁵. Above findings suggested that hepatic CYP7B1 potentially plays a vital role in obesity-related T2D in humans. In germ-free mice, hepatic CYP7A1 enzyme activity was mainly up-regulate²⁰. Gut microbiota-induced bile acid synthesis enzymes remodeling in liver differed between mice

and humans. Consistent with humans, antibiotic-treated hamsters displayed a higher relative expression level of hepatic *Cyp7b1*, but *Cyp7a1*, *Cyp8b1* and *Cyp27a1* relative mRNA levels remain unchanged. Moreover, hamsters displayed more similarities in bile acids metabolism and composition with human. Collectively, hamsters are more proper animals used for confirming whether modulation of gut microbiota-CYP7B1-bile acids axis is a potential therapeutic strategy for clinical T2D treatment.

In the gut, microbiota-derived enzymes mediated the complex biotransformations of bile acids produced in the liver, including deconjugation, 7-dehydroxylation and oxidation of hydroxyl groups⁵⁰. Bile acid deconjugation is carried out by BSH, expressed in *Lactobacilli*, *Bifidobacteria*, *Clostridium* and *Bacteroides*⁵¹⁻⁵³. Both the preferential reduction of the abundance of *Lactobacilli* and its BSH by the antioxidant tempol and the direct suppression

of BSH activity by caffeic acid phenethyl ester (CAPE) resulted in the accumulation of T β MCA in the ileum to ameliorate obesity and insulin resistance³⁵. Consistently, the levels of T β MCA in the ileum and feces were significantly elevated due to the absence of microbial BSH activity after antibiotic treatment in hamsters. Due to the markedly increased excretion in the feces of conjugated bile acids (Fig. S3C), such as TCA, GCA and GCDCA, the levels of these bile acids were not increased or even slightly decreased in the ileum (Fig. 4B). Collectively, the accumulation of T β MCA was due to both the upregulation of the alternative bile acid synthesis pathway and the inhibition of deconjugation. Secondary bile acids are generated by 7-dehydroxylation with microbial bile acid-inducible (*bai*) gene products. The antibiotic-treated hamsters had an overall reduction in secondary bile acids in the enterohepatic cycle, resulting from the lack of multiple 7-dehydroxylation steps.

FXR is a ligand-activated nuclear receptor that regulates bile acid homeostasis and is primarily expressed in the liver and gut⁵⁴. FXR can be bound by a variety of endogenous bile acids with various affinities, with the potency of FXR activation in reporter gene assays estimated at CDCA > LCA = DCA^{55,56}. The activated FXR signaling resulted in downregulated bile acid synthesis via the inhibition of the expression of CYP7A1⁵⁷. In contrast, the murine conjugated bile acid, T β MCA, was proven to be an endogenous FXR antagonist^{20,21}. It was verified that inhibition and knockout of intestinal FXR prevented obesity-related metabolic diseases in mice^{21–23}. In hamsters treated with antibiotics, intestinal FXR signaling (in humans and hamsters) was inhibited, associated with the increased T β MCA and the reduced DCA and LCA. However, there was no obvious difference in hepatic FXR signaling between vehicle- and antibiotic-treated hamsters. Thus, this revealed that modulation of bile acids by ablation of the gut microbiota mainly influenced intestinal FXR signaling in hamsters.

5. Conclusions

The present results highlighted that microbial modulation of bile acids was pivotal to regulating obesity-induced metabolic disorders in hamsters. It was suggested that removal of the gut microbiota mainly elevated alternative bile acid synthesis in the liver and suppressed the microbial deconjugation and dehydroxylation in the gut, leading to increased T β MCA and decreased secondary bile acids in the ileum. Remodeling of bile acid profiles due to antibiotic treatment had beneficial effects in improving glucose intolerance and hepatic steatosis. Furthermore, we found that intestinal FXR, but not hepatic FXR, was suppressed after antibiotic treatment in hamsters. These data support the view that intestinal FXR inhibition is a potential target for the clinical treatment of obesity-induced metabolic diseases.

Acknowledgments

We thank John J. Chiang for editing the manuscript. This work was supported by the National Key Research and Development Program of China (grant No. SQ2018YFC100236); the National Natural Science Foundation of China (grant Nos. 91857115, 81522007, 81470554, 31401011, and 81700010); the Fundamental Research Funds for the Central Universities: Clinical Medicine Plus X - Young Scholars Project of Peking University (grant No. PKU2018LCXQ013, China); and Beijing Nova Program (grant No. Z161100004916056, China).

Appendix A. Supporting information

Supporting data associated with this article can be found in the online version at <https://doi.org/10.1016/j.apsb.2019.02.004>.

References

1. Turnbaugh PJ, Ley RE, Mahowald MA, Magrini V, Mardis ER, Gordon JI. An obesity-associated gut microbiome with increased capacity for energy harvest. *Nature* 2006;**444**:1027–31.
2. Anhe FF, Roy D, Pilon G, Dudoine S, Matamoros S, Varin TV, et al. A polyphenol-rich cranberry extract protects from diet-induced obesity, insulin resistance and intestinal inflammation in association with increased *Akkermansia* spp. population in the gut microbiota of mice. *Gut* 2015;**64**:872–83.
3. Forslund K, Hildebrand F, Nielsen T, Falony G, Le Chatelier E, Sunagawa S, et al. Disentangling type 2 diabetes and metformin treatment signatures in the human gut microbiota. *Nature* 2015;**528**:262–6.
4. Leung C, Rivera L, Furness JB, Angus PW. The role of the gut microbiota in NAFLD. *Nat Rev Gastroenterol Hepatol* 2016;**13**:412–25.
5. Gu Y, Wang X, Li J, Zhang Y, Zhong H, Liu R, et al. Analyses of gut microbiota and plasma bile acids enable stratification of patients for antidiabetic treatment. *Nat Commun* 2017;**8**:1785.
6. Wu H, Esteve E, Tremaroli V, Khan MT, Caesar R, Manneras-Holm L, et al. Metformin alters the gut microbiome of individuals with treatment-naïve type 2 diabetes, contributing to the therapeutic effects of the drug. *Nat Med* 2017;**23**:850–8.
7. Zhang X, Zhao Y, Xu J, Xue Z, Zhang M, Pang X, et al. Modulation of gut microbiota by berberine and metformin during the treatment of high-fat diet-induced obesity in rats. *Sci Rep* 2015;**5**:14405.
8. Sun L, Xie C, Wang G, Wu Y, Wu Q, Wang X, et al. Gut microbiota and intestinal FXR mediate the clinical benefits of metformin. *Nat Med* 2018;**24**:1919–29.
9. Kovatcheva-Datchary P, Nilsson A, Akrami R, Lee YS, De Vadder F, Arora T, et al. Dietary fiber-induced improvement in glucose metabolism is associated with increased abundance of *Prevotella*. *Cell Metab* 2015;**22**:971–82.
10. Le Chatelier E, Nielsen T, Qin J, Prifti E, Hildebrand F, Falony G, et al. Richness of human gut microbiome correlates with metabolic markers. *Nature* 2013;**500**:541–6.
11. Schroeder BO, Backhed F. Signals from the gut microbiota to distant organs in physiology and disease. *Nat Med* 2016;**22**:1079–89.
12. Albaugh VL, Flynn CR, Cai S, Xiao Y, Tamboli RA, Abumrad NN. Early increases in bile acids post Roux-en-Y gastric bypass are driven by insulin-sensitizing, secondary bile acids. *J Clin Endocrinol Metab* 2015;**100**:E1225–33.
13. Kars M, Yang L, Gregor MF, Mohammed BS, Pietka TA, Finck BN, et al. Tauroursodeoxycholic acid may improve liver and muscle but not adipose tissue insulin sensitivity in obese men and women. *Diabetes* 2010;**59**:1899–905.
14. Zhu Y, Liu H, Zhang M, Guo GL. Fatty liver diseases, bile acids, and FXR. *Acta Pharm Sin B* 2016;**6**:409–12.
15. Worthmann A, John C, Ruhlemann MC, Baguhl M, Heinsen FA, Schaltenberg N, et al. Cold-induced conversion of cholesterol to bile acids in mice shapes the gut microbiome and promotes adaptive thermogenesis. *Nat Med* 2017;**23**:839–49.
16. Matsubara T, Li F, Gonzalez FJ. FXR signaling in the enterohepatic system. *Mol Cell Endocrinol* 2013;**368**:17–29.
17. Peng L, Piekos S, Guo GL, Zhong XB. Role of farnesoid X receptor in establishment of ontogeny of phase-I drug metabolizing enzyme genes in mouse liver. *Acta Pharm Sin B* 2016;**6**:453–9.
18. Degirolamo C, Rainaldi S, Bovenga F, Murzilli S, Moschetta A. Microbiota modification with probiotics induces hepatic bile acid synthesis via down-regulation of the FXR-FGF15 axis in mice. *Cell Rep* 2014;**7**:12–8.
19. Wahlstrom A, Sayin SI, Marschall HU, Backhed F. Intestinal crosstalk between bile acids and microbiota and its impact on host metabolism. *Cell Metab* 2016;**24**:41–50.

20. Sayin SI, Wahlstrom A, Felin J, Jantti S, Marschall HU, Bamberg K, et al. Gut microbiota regulates bile acid metabolism by reducing the levels of tauro- β -muricholic acid, a naturally occurring FXR antagonist. *Cell Metab* 2013;**17**:225–35.
21. Gonzalez FJ, Jiang C, Patterson AD. An intestinal microbiota-farnesoid X receptor axis modulates metabolic disease. *Gastroenterology* 2016;**151**:845–59.
22. Jiang C, Xie C, Li F, Zhang L, Nichols RG, Krausz KW, et al. Intestinal farnesoid X receptor signaling promotes nonalcoholic fatty liver disease. *J Clin Invest* 2015;**125**:386–402.
23. Jiang C, Xie C, Lv Y, Li J, Krausz KW, Shi J, et al. Intestine-selective farnesoid X receptor inhibition improves obesity-related metabolic dysfunction. *Nat Commun* 2015;**6**:10166.
24. Gardes C, Chaput E, Staempfli A, Blum D, Richter H, Benson GM. Differential regulation of bile acid and cholesterol metabolism by the farnesoid X receptor in *Ldlr*^{-/-} mice versus hamsters. *J Lipid Res* 2013;**54**:1283–99.
25. Haidari M, Leung N, Mahbub F, Uffelman KD, Kohen-Avramoglu R, Lewis GF, et al. Fasting and postprandial overproduction of intestinally derived lipoproteins in an animal model of insulin resistance. Evidence that chronic fructose feeding in the hamster is accompanied by enhanced intestinal *de novo* lipogenesis and ApoB48-containing lipoprotein overproduction. *J Biol Chem* 2002;**277**:31646–55.
26. Gao S, He L, Ding Y, Liu G. Mechanisms underlying different responses of plasma triglyceride to high-fat diets in hamsters and mice: roles of hepatic MTP and triglyceride secretion. *Biochem Biophys Res Commun* 2010;**398**:619–26.
27. Briand F, Thiebtemont Q, Muzotte E, Sulpice T. High-fat and fructose intake induces insulin resistance, dyslipidemia, and liver steatosis and alters *in vivo* macrophage-to-feces reverse cholesterol transport in hamsters. *J Nutr* 2012;**142**:704–9.
28. Basciano H, Miller AE, Naples M, Baker C, Kohen R, Xu E, et al. Metabolic effects of dietary cholesterol in an animal model of insulin resistance and hepatic steatosis. *Am J Physiol Endocrinol Metab* 2009;**297**:E462–73.
29. Dong B, Kan CF, Singh AB, Liu J. High-fructose diet down-regulates long-chain acyl-CoA synthetase 3 expression in liver of hamsters via impairing LXR/RXR signaling pathway. *J Lipid Res* 2013;**54**:1241–54.
30. Chevalier C, Stojanovic O, Colin DJ, Suarez-Zamorano N, Tarallo V, Veyrat-Durebex C, et al. Gut microbiota orchestrates energy homeostasis during cold. *Cell* 2015;**163**:1360–74.
31. Thomas C, Pellicciari R, Pruzanski M, Auwerx J, Schoonjans K. Targeting bile-acid signalling for metabolic diseases. *Nat Rev Drug Discov* 2008;**7**:678–93.
32. Haeusler RA, Astiarraga B, Camastra S, Accili D, Ferrannini E. Human insulin resistance is associated with increased plasma levels of 12 α -hydroxylated bile acids. *Diabetes* 2013;**62**:4184–91.
33. Jiao N, Baker SS, Chapa-Rodriguez A, Liu W, Nugent CA, Tsompana M, et al. Suppressed hepatic bile acid signalling despite elevated production of primary and secondary bile acids in NAFLD. *Gut* 2018;**67**:1881–91.
34. Heuman DM. Quantitative estimation of the hydrophilic-hydrophobic balance of mixed bile salt solutions. *J Lipid Res* 1989;**30**:719–30.
35. Xie C, Jiang C, Shi J, Gao X, Sun D, Sun L, et al. An intestinal farnesoid X receptor–ceramide signaling axis modulates hepatic gluconeogenesis in mice. *Diabetes* 2017;**66**:613–26.
36. Despres JP, Lemieux I. Abdominal obesity and metabolic syndrome. *Nature* 2006;**444**:881–7.
37. Jin W, Cui B, Li P, Hua F, Lv X, Zhou J, et al. 1,25-Dihydroxyvitamin D3 protects obese rats from metabolic syndrome via promoting regulatory T cell-mediated resolution of inflammation. *Acta Pharm Sin B* 2018;**8**:178–87.
38. Liu Q, Liu S, Gao L, Sun S, Huan Y, Li C, et al. Anti-diabetic effects and mechanisms of action of a Chinese herbal medicine preparation JQ-R *in vitro* and in diabetic KK^{Ay} mice. *Acta Pharm Sin B* 2017;**7**:461–9.
39. Tang Y, Zhang X, Chen Z, Yin W, Nan G, Tian J, et al. Novel benzamido derivatives as PTP1B inhibitors with anti-hyperglycemic and lipid-lowering efficacy. *Acta Pharm Sin B* 2018;**8**:919–32.
40. Wang S, Wu C, Li X, Zhou Y, Zhang Q, Ma F, et al. Syringaresinol-4-O- β -D-glucoside alters lipid and glucose metabolism in HepG2 cells and C2C12 myotubes. *Acta Pharm Sin B* 2017;**7**:453–60.
41. Liu J, Wang Y, Lin L. Small molecules for fat combustion: targeting obesity. *Acta Pharm Sin B* 2018. Available from: <https://doi.org/10.1016/j.apsb.2018.09.007>.
42. Sonnenburg JL, Backhed F. Diet-microbiota interactions as moderators of human metabolism. *Nature* 2016;**535**:56–64.
43. Khoruts A, Sadowsky MJ. Understanding the mechanisms of faecal microbiota transplantation. *Nat Rev Gastroenterol Hepatol* 2016;**13**:508–16.
44. Khoruts A. Faecal microbiota transplantation in 2013: developing human gut microbiota as a class of therapeutics. *Nat Rev Gastroenterol Hepatol* 2014;**11**:79–80.
45. Hegazy AN, West NR, Stubbington MJT, Wendt E, Suijker KIM, Datsi A, et al. Circulating and tissue-resident CD4⁺ T cells with reactivity to intestinal microbiota are abundant in healthy individuals and function is altered during inflammation. *Gastroenterology* 2017;**153**:1320–37. e16.
46. Yu AM, Ingelman-Sundberg M, Cherrington NJ, Aleksunes LM, Zanger UM, Xie W, et al. Regulation of drug metabolism and toxicity by multiple factors of genetics, epigenetics, lncRNAs, gut microbiota, and diseases: a meeting report of the 21st International Symposium on Microsomes and Drug Oxidations (MDO). *Acta Pharm Sin B* 2017;**7**:241–8.
47. Takahashi S, Fukami T, Masuo Y, Brocker CN, Xie C, Krausz KW, et al. CYP2C70 is responsible for the species difference in bile acid metabolism between mice and humans. *J Lipid Res* 2016;**57**:2130–7.
48. Wang DQ, Tazuma S, Cohen DE, Carey MC. Feeding natural hydrophilic bile acids inhibits intestinal cholesterol absorption: studies in the gallstone-susceptible mouse. *Am J Physiol Gastrointest Liver Physiol* 2003;**285**:G494–502.
49. Ferrell JM, Boehme S, Li F, Chiang JY. Cholesterol 7 α -hydroxylase-deficient mice are protected from high-fat/high-cholesterol diet-induced metabolic disorders. *J Lipid Res* 2016;**57**:1144–54.
50. Ussar S, Griffin NW, Bezy O, Fujisaka S, Vienberg S, Softic S, et al. Interactions between gut microbiota, host genetics and diet modulate the predisposition to obesity and metabolic syndrome. *Cell Metab* 2015;**22**:516–30.
51. Ridlon JM, Kang DJ, Hylemon PB. Bile salt biotransformations by human intestinal bacteria. *J Lipid Res* 2006;**47**:241–59.
52. Jones BV, Begley M, Hill C, Gahan CG, Marchesi JR. Functional and comparative metagenomic analysis of bile salt hydrolase activity in the human gut microbiome. *Proc Natl Acad Sci U S A* 2008;**105**:13580–5.
53. Joyce SA, MacSharry J, Casey PG, Kinsella M, Murphy EF, Shanahan F, et al. Regulation of host weight gain and lipid metabolism by bacterial bile acid modification in the gut. *Proc Natl Acad Sci U S A* 2014;**111**:7421–6.
54. Lefebvre P, Cariou B, Lien F, Kuipers F, Staels B. Role of bile acids and bile acid receptors in metabolic regulation. *Physiol Rev* 2009;**89**:147–91.
55. Makishima M, Okamoto AY, Repa JJ, Tu H, Learned RM, Luk A, et al. Identification of a nuclear receptor for bile acids. *Science* 1999;**284**:1362–5.
56. Parks DJ, Blanchard SG, Bledsoe RK, Chandra G, Consler TG, Kliewer SA, et al. Bile acids: natural ligands for an orphan nuclear receptor. *Science* 1999;**284**:1365–8.
57. Gonzalez FJ, Jiang C, Bisson WH, Patterson AD. Inhibition of farnesoid X receptor signaling shows beneficial effects in human obesity. *J Hepatol* 2015;**62**:1234–6.